A Stochastic Mixed Integer Linear Programming Formulation for the Balancing Energy Activation Problem under Uncertainty

Martin Håberg
Gerard Doorman
Dept. of Electric Power Engineering
Norwegian University of Science and Technology
Trondheim, Norway
martin.haberg@ntnu.no

***Abstract*—In the activation market, the Transmission System Operator selects and activates balancing energy bids to cover the system imbalance. Growing use of intermittent energy sources increases uncertainty in system operation and new EU regulations, including a so-called Activation Optimization Function and new Standard Products for manual frequency restoration reserves (mFRR), will change the activation process significantly. However, commonly used price-based bid selection approaches are incapable of taking intertemporal constraints and uncertainty into account in the activation process.**

This paper presents a new optimization formulation, built on stochastic unit commitment principles, using imbalance forecast scenarios to propose bid activation schedules minimizing expected activation costs. Unlike earlier approaches, intertemporal characteristics of the proposed mFRR product are modeled in detail.

The optimization procedure is implemented in a rolling horizon simulation and demonstrated using Norwegian imbalance and market data. Compared to a corresponding deterministic approach, the stochastic strategy significantly reduces activation costs.

***Index Terms*—optimal scheduling, power generation dispatch, power system modeling, stochastic processes**

NOMENCLATURE

Indices

a	aFRR price step
b	Balancing bid
s	Imbalance scenario
t, τ	Time period

Parameters

ω_{ts}	Predicted imbalance in time period t in scenario s
$\overline{X}_b$	Capacity of mFRR bid b
$\overline{Y}_a$	Capacity of aFRR price step a
π_s	Probability of imbalance scenario s
C_a^{aFRR}	Activation cost of aFRR at price step a
C_b^{mFRR}	Activation cost for mFRR bid b

Sets

$\mathcal{A}$	Set of aFRR price steps
$\mathcal{B}$	Set of all mFRR bids
$\mathcal{S}$	Set of all imbalance scenarios
$\mathcal{T}$	Set of all time periods

Variables

u_{bts}	Commitment status of mFRR bid b in time period t and scenario s (binary)
v_{bts}	Indicates bid b starts delivery in time period t and scenario s (binary)
x_{bts}	Delivery power from bid b in time period t and scenario s
x_{bts}^R	Ramping power from bid b in time period t and scenario s
x_{bts}^S	Delivery setpoint for bid b in time period t and scenario s
y_{ats}	Activated aFRR from price step a in time period t and scenario s

Specifiers

$^+$	Upward direction
$^-$	Downward direction

I. INTRODUCTION

The instantaneous balance between generation and consumption in the power system must be monitored and adjusted. This is among the operational responsibilities of the Transmissoin System Operator (TSO), and adjustments are made by activating balancing energy from reserves, either provided by generating units with spinning reserve capacity or fast-start capability, or by dispatchable consumption.

Through the balancing energy activation market, the TSO aims at utilizing these reserves efficiently. Balancing Service Providers (BSPs) submit bids for balancing energy products, which will be activated by the TSO in the order of bid price until the imbalance between generation and consumption is covered. In Europe, balancing energy is activated from Frequency Restoration Reserves (FRR), which can be manually (mFRR) or automatically (aFRR) activated, or by Replacement Reserves (RR), used to relieve FRR activation for longer, persisting imbalances. While the activation of aFRR can respond to a disturbance within a few minutes, mFRR can typically need 15 minutes (and for RR, even more) before delivering the requested amount of power. And while aFRR

follows a control error based on frequency and cross-border flows, manual activations are subject to operator decisions and can also be used *proactively* to cover an expected future imbalance [1].

Following significant progress in the integration of European day-ahead and intraday markets for electricity, balancing markets are currently also in the process of integration as a step towards the vision of an internal energy market. Due to differing market rules and operational practices among Transmission System Operators (TSOs), harmonization is necessary in order to create a level playing field for market participants [2]. The European Network of Transmission System Operators for Electricity (ENTSO-E) is developing new Network Codes, the rules and regulations for European power markets, including the Guideline on Electricity Balancing [3] aims to increase pan-European welfare through secure and efficient balancing operations. The Guideline requires the development of a set of *Standard Products* to be shared among TSOs and used for the exchange of balancing energy. Although several proposals have been made, the exact specifications of these products are still under discussion. The activation of balancing energy is to be governed by an *Activation Optimization Function*, the specifications of which are also still to be decided.

Several studies have been made on the integration of balancing markets, many including models of the balancing energy activation market [4]–[10]. Other notable approaches include [11] and [12]. As they are often used in long-horizon simulations, they do not model the bid selection optimization using detailed the product specifications, which requires modelling the operating states and restrictions on duration and ramping, as is done in the unit commitment problem [13].

Increasing share of power generation from intermittent renewable sources increases uncertainty on all time scales, and stochastic unit commitment [14], is a method managing uncertainty through scenario representations which has been used for day-ahead scheduling optimizations, but the technique has not seen widespread use in balancing energy operations.

This paper provides a formulation of the balancing energy activation problem, taking uncertainty into account through a stochastic optimization approach and representing the opportunities and limitations provided by mFRR Standard Products in greater detail. The optimization model is presented in Section II, together with the description of a case study based on a simplified representation of the Norwegian system, disregarding network constraints. Section III presents results and findings from the case study simulations, while their validity and implications are discussed in Section IV. Section V lists some of the most important conclusions.

II. Methodology

A. Model Formulation

The balancing energy activation model takes into account the history of previous bid activations, the current imbalance situation and expectations of the future imbalance to propose a an optimal schedule for each available mFRR bid in the market. The optimization routine is then re-run at regular intervals, e.g. every 5 minutes, using updated imbalance information and forecasts. The optimization does not provide a control signal for the aFRR, but includes a representation of the expected aFRR response to the mFRR activation and imbalance situation. The objective in (1) is to minimize the expected costs from activation of mFRR and aFRR over the scheduling horizon.

$$\min \sum_{s\in\mathcal{S}} \pi_s \sum_{t\in\mathcal{T}} \left(\sum_{a\in\mathcal{A}} C_a^{\text{aFRR}} y_{ats} + \sum_{b\in\mathcal{B}} C_b^{\text{mFRR}} x_{bts} \right) \tag{1}$$

The model formulation uses 5 minute timesteps and distinguishes between mFRR power output during the delivery period, for which the cost is reflected in the objective function, and during the ramping period, x^R_{bts}. This energy is delivered before the bid is fully activated and contributes to the power balance, but without driving activation costs. Ramping constraints are disregarded for aFRR due to its fast-ramping capability. The sum of power from mFRR and aFRR schedules must equal the imbalance forecasts ω_{ts} for each time period and scenario, as given in (2), which includes both upward and downward activations:

$$\begin{aligned} &\sum_{b\,\in\mathcal{B}^+} (x_{bts} + x^R_{bts}) - \sum_{b\,\in\mathcal{B}^-} (x_{bts} + x^R_{bts}) \\ &\quad + \sum_{a\,\in\mathcal{A}} (y^+_{ats} - y^-_{ats}) = \omega_{ts} \qquad \forall t, s \end{aligned} \tag{2}$$

Power from aFRR is limited only by the available capacities, while delivery and ramping power from mFRR depends on the commitment status u_{bts} of the bid:

$$x_{bts} \le \overline{X}_b u_{bts} \qquad \forall b, t, s \tag{3}$$
$$x^R_{bts} \le \overline{X}_b (1 - u_{b\tau s}) \tau = t-1, t \quad \forall b, t, s \tag{4}$$
$$y^+_{ats} \le \overline{Y}_a \qquad \forall a, t, s \tag{5}$$
$$y^-_{ats} \le \overline{Y}_a \qquad \forall a, t, s \tag{6}$$

The mFRR activation is also subject to a set of ramping, duration and other operating constraints, some of which use the binary startup indicator variable v_{bts} or the variable x^S_{bst} which defines the requested power level at the beginning of a delivery period. Then, for all b, t, s,

$$v_{bts} \geq u_{bts} - u_{b(t-1)s} \tag{7}$$
$$v_{bts} \leq 1 - v_{b(t-1)s} - v_{b(t-2)s} \tag{8}$$
$$v_{bts} \leq x_{b(t-2)s} + x^R_{b(t-2)s} \tag{9}$$
$$x^S_{bts} \leq v_{bts} \tag{10}$$
$$x^R_{bts} \leq \overline{X}_b(1 - v_{b(t+3)s}) \tag{11}$$
$$x^R_{bts} \leq \overline{X}_b\left(\frac{2}{3}x^S_{b(t+1)s} + \frac{1}{3}x^S_{b(t+2)s}\right) \tag{12}$$
$$x^R_{bts} \geq \frac{2}{3}\overline{X}_b(x^S_{b(t+1)s} - u_{bts}) \tag{13}$$
$$x^R_{bts} \geq \frac{1}{3}\overline{X}_b(x^S_{b(t+2)s} - u_{bts}) \tag{14}$$
$$x_{bts} \geq \overline{X}_b x^S_{b\tau s} \qquad \tau = t-3, ..., t \tag{15}$$
$$x_{bts} \leq \overline{X}_b \sum_{\tau=t-3}^{t} x^S_{b\tau s} \tag{16}$$
$$x_{bts} \leq x_{b(t-1)s} + \overline{X}_b(1 - v_{b(t-1)s}) \tag{17}$$
$$x_{bts} \leq x_{b(t+1)s} + \overline{X}_b(1 - v_{bts}) \tag{18}$$
$$x_{bts} \leq x_{b(t-1)s} + x^R_{b(t-1)s} - x^R_{bts} + \frac{1}{3}\overline{X}_b \tag{19}$$
$$\sum_{\tau=t}^{t+7} u_{b\tau s} \leq 7 \tag{20}$$

Eq. (10) requires a nonzero value for the binary decision variable v_{bts} for a new delivery period to start. This is ensured by (7) when the commmitment status changes, and (8) prevents prematurely starting a new delivery periods. Eq. (9) requires the delivery period to be preceded either by ramping or an earlier delivery period. Eqs. (11)-(14) govern the amount of ramping power, which is related to the capacity limit $\overline{X}_b$ and the delivery power setpoint $x^S_{b\tau s}$ in subsequent periods τ, e.g. setting ramping power to $\frac{1}{3}$ of the delivery power setpoint 5 minutes into the ramping period through (12) and (14). Eqs. (15)-(19) ensure delivery power x_{bts} mathes the setpoint, preventing change of output between periods unless a new delivery period is started (17)-(18), and (19) limits the ramp rate when such change is allowed. Eq. (20) sets a maximum duration of for the delivery period of an activated bid.

Non-anticipativity constaints require first-stage decision variables to take the same value across all scenarios before the realization of uncertain parameters. For a scenario fan, this only applies to $t = 1$.

$$u_{bts} = u_{bt\sigma} \qquad \sigma \neq s, \forall b, t, s \tag{21}$$
$$v_{bts} = v_{bt\sigma} \qquad \sigma \neq s, \forall b, t, s \tag{22}$$
$$x_{bts} = x_{bt\sigma} \qquad \sigma \neq s, \forall b, t, s \tag{23}$$
$$x^R_{bts} = x^R_{bt\sigma} \qquad \sigma \neq s, \forall b, t, s \tag{24}$$
$$x^S_{bts} = x^S_{bt\sigma} \qquad \sigma \neq s, \forall b, t, s \tag{25}$$

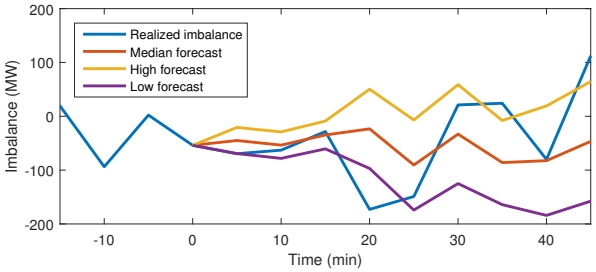

Fig. 1. Imbalance forecast scenarios and actual imbalance realization over a scheduling horizon

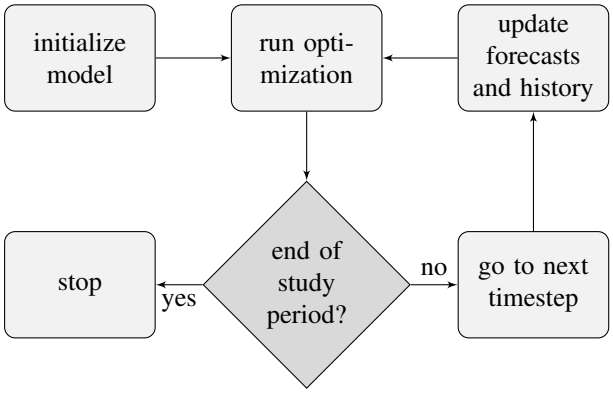

Fig. 2. Implemented rolling horizon simulation procedure

Finally, we require variables to be non-negative or binary

$$x_{bts}, x^R_{bts}, x^S_{bts} \geq 0 \qquad \forall b, t, s \tag{26}$$
$$y^+_{ats}, y^-_{ats} \geq 0 \qquad \forall a, t, s \tag{27}$$
$$u_{bts}, v_{bts} \in \{0, 1\} \qquad \forall b, t, s \tag{28}$$

Note that the formulation includes no network representation, thereby disregarding congestion and losses.

B. Model Implementation

Uncertainty in the future imbalance is represented by three scenarios in a scenario fan (cf. Fig 1), thus the model is a two-stage problem with fixed recourse, and can be solved readily using deterministic equivalents. For each re-optimization, the scheduling horizon is 45 minutes ahead, as intraday markets further ahead are not yet closed. Then, for each timestep in the study period, the actual aFRR and mFRR output can be found as the *final plan*, given at $t = 0$ in each timestep iteration. Here, the mFRR output will be a sunk decision, while the aFRR power will be chosen by the optimizer to satisfy the power balance considering actual realized imbalance.

The model has been implemented in Xpress-Mosel[1] together with a file framework for rolling horizon simulations, cf. Fig. 2. Simulations were run on an Intel Core i7-6600U laptop computer with 16 GB RAM.

[1]FICO®Xpress Optimization Suite v7.9

C. Case Study Specifications

For the purpose of demonstrating the stochastic strategy, the activation process was simulated for 18 consecutive time periods, corresponding to 90 minutes of balancing operation, and compared against a corresponding deterministic strategy. For the imbalance realizations, Norwegian imbalance data from June 16, 2016 were used. The imbalance forecasts were generated from percentiles of probability distributions based on historical imbalance data series, with probabilities calculated from a calibration of the forecasts against the realized imbalance on a training data set. Fig. 1 shows the realized imbalance and forecasts used by the model for a specific time period in the simulation.

A list of 16 balancing activation bids for mFRR were created based on prices and volumes in the Norwegian balancing energy market, eight in each direction of power delivery. The activation market for aFRR is yet to be introduced in the Nordic system, hence activation prices are uncertain. When aFRR prices are similar to or lower than mFRR prices, automatic activations will be preferential due to shorter activation time and flexible output levels. Manual activations will only be rational when there is insufficient aFRR to cover the imbalance. In this case study, the majority of aFRR is assumed to have a higher activation price than mFRR, causing proactive activations of mFRR to minimize expected activation costs. A simple stepwise cost curve is assumed, resulting in the supply curve in Fig. 3.

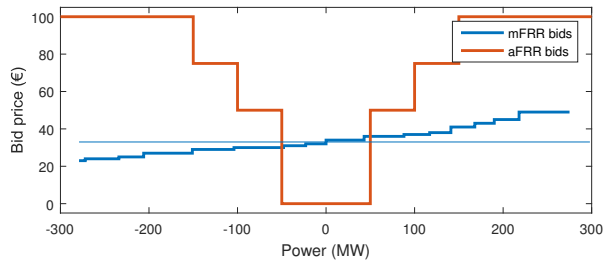

Fig. 3. Supply curve of upward and downward mFRR and aFRR capacity

III. Results

A. Activation Costs

Fig. 4 shows the realized activation costs for the stochastic and deterministic optimization strategies in each 5 minute period during the simulated case study. Although activation costs are lower with the deterministic strategy during some periods, it is outperformed over the 90 minute study period, with total activation costs equalling 7 364 € in the deterministic case, 18 % higher than 6 035 € for the stochastic approach. Sensitivity analyses were run using different aFRR price curves. When almost the entire amount (290 of 300 MW in each direction) of aFRR is priced at 100 €, activation costs increase to 17 491 € (det.), 9 % higher than 16 084 € (stoch.). For low aFRR prices, the optimizer prefers to wait-and-see, rather than activate mFRR in advance. This leads to inadequate response

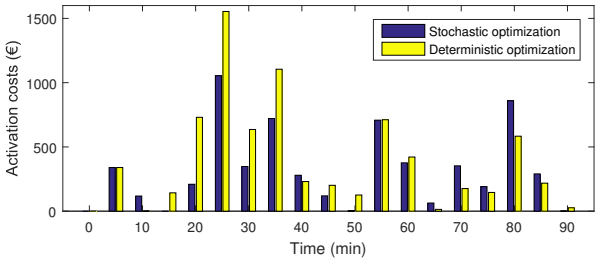

Fig. 4. Activation costs for each simulated time period with the stochastic and deterministic strategies

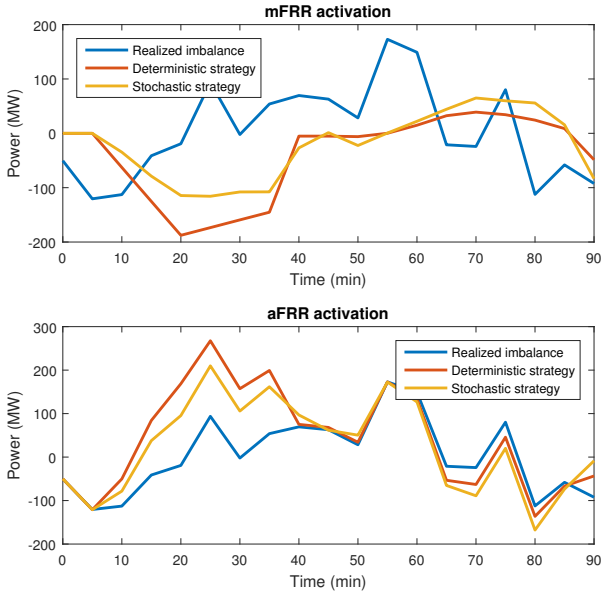

Fig. 5. Net activation volumes for mFRR and aFRR over the simulation horizon

in several cases when the imbalance turns out to deviate from the forecast.

B. Reserve Activation

Fig. 5 shows how the net activated mFRR and aFRR (i.e. upward minus downward) volumes differ under the two optimization strategies. The most prominent deviations between strategies occur in the period $t = 10 - 35$, where mFRR and aFRR are activated in opposite directions due to a significant forecast error.

The composition of upward and downward activations also differs between the strategies. Fig. 6 indicates the schedules proposed in one of the re-optimizations. Here, the deterministic strategy proposes activating both upward and downward reserves simultaneously to deal with imbalance fluctuations, while the stochastic approach proposes using more aFRR.

C. Running Times

For the optimization runs in the case study (cf. II-C), the solver is able to identify near-optimal solutions within a few

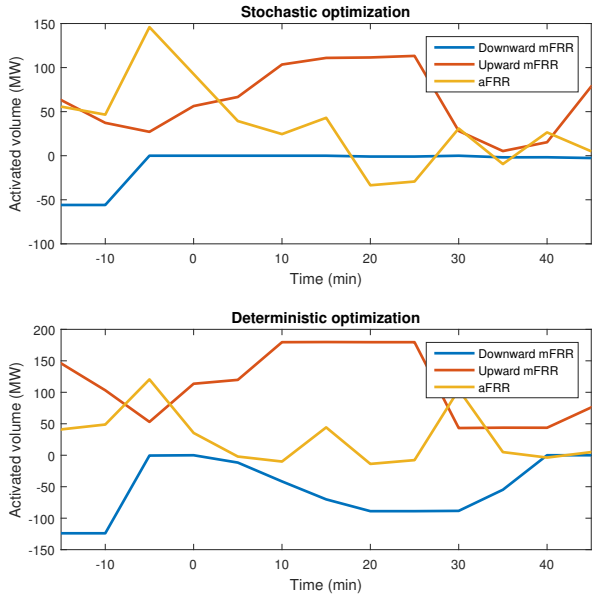

Fig. 6. Upward and downward activation volumes under different strategies

TABLE I
SIMULATION RUNNING TIMES FOR STOCHASTIC MODEL

Duality gap	Median	75th pct.	Max	Max, det. model
5 %	6 sec	10 sec	34 sec	4 sec
2 %	12 sec	44 sec	>5 min	9 sec
1 %	40 sec	160 sec	>5 min	33 sec

seconds. As Table I indicates, however, there are significant differences in running time between different time periods, and in a few cases the solver needs more than one minute to reduce the duality gap below 2 %. The deterministic model is notably quicker. It should be noted that most of the time and effort used for closing the duality gap is related to improving the lower bound, while optimal decisions are often found almost immediately using built-in heuristics in the solver. In other words, the additional running time required to converge rarely improves the quality of the solution by a significant amount.

Sensitivity analyses indicate the running time increasing with the scheduling horizon, number of bids and imbalance forecast scenarios, all of which will increase the number of binary variables. Running time was also found to decrease with increasing amounts of low-priced aFRR available.

IV. Discussion

While the case study indicates potential cost savings from using a stochastic activation strategy, the added benefit depends on the relation between mFRR and aFRR bid prices. Higher aFRR prices increase activation costs, not only from forecast errors, but also from a shift towards more mFRR activations. On the other hand, a comparatively low aFRR price removes the incentive to schedule mFRR proactively.

Assuming perfect information, the deterministic strategy proposes minimum-cost schedules, sometimes including simultaneous upward and downward activations of mFRR to closely match the imbalance forecast profile. The deterministic strategy has no incentive to propose flexible schedules that easily adapt to unexpected imbalance realizations. The simulation reveals the consequence of overestimating the quality of the forecast. The stochastic optimization, on the other hand, proposes a *compromise schedule* which is not optimal for any forecast scenario, but it appears to be less vulnerable to forecast errors than the deterministic strategy.

Using the bid prices in the activation market, it is possible to cross-optimize between mFRR and aFRR using a proactive philosophy. While this can reduce activation costs, Fig. 5 gives, however, a clear illustration of a *proactive failure*, where the imbalance takes a different turn than expected, and the aFRR must cover not only the imbalance, but also the mFRR recently activated in the opposite direction.

For an optimization procedure to be applied in real-time balancing operations, computational speed is crucial. Both the Standard Product representation and imbalance forecast scenarios significantly add to the complexity of the problem. The case study simulations show that near-optimal solutions can be found quickly. However, real-life balancing energy activation markets not only include more bid providers, but there may also be network constraints or other considerations to take into account in the bid selection process, increasing the running time of the algorithm. Still, there are ways to improve the computational performance, including parallel computing and faster hardware. Other options include using tailored heuristics or a progressive hedging algorithm [15] or another dual decomposition approach [16].

V. Conclusions

An optimization model has been developed to find minimum cost solutions to the balancing energy activation problem. It uses bid data and imbalance forecasts, includes a detailed representation of an mFRR Standard Product and takes uncertainty into account through a scenario representation. Moderately-sized problem instances can be solved to near-optimality in a few seconds, and opportunities for improving the computational performance have been identified.

Case study simulations based on data from the Norwegian power system show a substantial reduction in activation costs by taking uncertainty into account in the optimization. The cost savings depend on the relative price differences between the mFRR and aFRR product, as well as the quality of the imbalance forecasts.

Simulations also demonstrate the interaction between aFRR and proactive activation of mFRR, including a *proactive failure*, where a considerable amount of balancing energy is activated in the upward and downward directions simultaneiously due to forecast error.

References

[1] M. Haberg and G. Doorman, "Classification of balancing markets based on different activation philosophies: proactive and reactive designs," in *2016 13th International Conference on the European Energy Market (EEM)*, IEEE, Jun. 2016, pp. 1–5.

[2] R. A. C. van der Veen, G. Doorman, O. S. Grande, A. Abbasy, R. A. Hakvoort, F. Nobel, and D. A. M. Klaar, "Harmonization and integration of national balancing markets in europe – regulatory challenges," in *Cigre session 43*, Paris, France, 2010.

[3] European Commission, *Guideline on electricity balancing, v. 24.01.2017*, 2016.

[4] A. Abbasy, R. A. C. van der Veen, and R. A. Hakvoort, "Effect of integrating regulating power markets of northern europe on total balancing costs," in *2009 IEEE Bucharest PowerTech*, IEEE, Jun. 2009, pp. 1–7.

[5] S. Jaehnert and G. Doorman, "Modelling an integrated northern european regulating power market based on a common day-ahead market," *Proc. of IAEE International Conference, Rio de ...*, pp. 1–17, 2010.

[6] ——, "Assessing the benefits of regulating power market integration in northern europe," *International Journal of Electrical Power & Energy Systems*, vol. 43, no. 1, pp. 70–79, Dec. 2012.

[7] T. Aigner, S. Jaehnert, G. Doorman, and T. Gjengedal, "The effect of large-scale wind power on system balancing in northern europe," *IEEE Transactions on Sustainable Energy*, vol. 3, no. 4, pp. 751–759, 2012.

[8] H. Farahmand, T. Aigner, G. Doorman, M. Korpas, and D. Huertas-Hernando, "Balancing market integration in the northern european continent: a 2030 case study," *IEEE Transactions on Sustainable Energy*, vol. 3, no. 4, pp. 918–930, Oct. 2012.

[9] Y. Gebrekiros and G. Doorman, "Balancing energy market integration in northern europe — modeling and case study," in *2014 IEEE PES General Meeting — Conference & Exposition*, IEEE, Jul. 2014, pp. 1–5.

[10] Y. Gebrekiros, G. Doorman, S. Jaehnert, and H. Farahmand, "Balancing energy market integration considering grid constraints," in *2015 IEEE Eindhoven PowerTech*, IEEE, Jun. 2015, pp. 1–6.

[11] R. A. C. van der Veen, A. Abbasy, and R. a. Hakvoort, "An agent-based analysis of main cross-border balancing arrangements for northern europe," in *2011 IEEE Trondheim PowerTech*, IEEE, Jun. 2011, pp. 1–8.

[12] J. D. Sprey, T. Drees, D. vom Stein, and A. Moser, "Impact of balancing energy on network congestions," in *2015 12th International Conference on the European Energy Market (EEM)*, IEEE, May 2015, pp. 1–6.

[13] M. Carrión and J. M. Arroyo, "A computationally efficient mixed-integer linear formulation for the thermal unit commitment problem," *Power Systems, IEEE Transactions on*, vol. 21, no. 3, pp. 1371–1378, 2006.

[14] S. Takriti, J. Birge, and E. Long, "A stochastic model for the unit commitment problem," *IEEE Transactions on Power Systems*, vol. 11, no. 3, pp. 1497–1508, 1996.

[15] R. T. Rockafellar and R. J. B. Wets, "Scenarios and policy aggregation in optimization under uncertainty," *Mathematics of Operations Research*, vol. 16, no. 1, pp. 119–147, 1991.

[16] K. Kim and V. M. Zavala, "Large-scale stochastic mixed-integer programming algorithms for power generation scheduling," in *Alternative Energy Sources and Technologies*, M. Martín, Ed., Cham: Springer International Publishing, 2016, pp. 493–512.